coatings

Article

Investigation of Multi-Mesa-Channel-Structured AlGaN/GaN MOSHEMTs with SiO_2 Gate Oxide Layer

Jhang-Jie Jian [1], Hsin-Ying Lee [2], Edward-Yi Chang [3] and Ching-Ting Lee [1,2,4,*]

1 Institute of Microelectronics, Department of Electrical Engineering, National Cheng Kung University, Tainan 701, Taiwan; zxcg61116@gmail.com
2 Department of Photonics, National Cheng Kung University, Tainan 701, Taiwan; hylee@ee.ncku.edu.tw
3 Department of Materials Science and Engineering, National Yang Ming Chiao Tung University, Hsinchu 300, Taiwan; edc@mail.nctu.edu.tw
4 Department of Electrical Engineering, Yuan Ze University, Taoyuan 320, Taiwan
* Correspondence: ctlee@ee.ncku.edu.tw; Tel.: +886-6-2082-368

Abstract: In this study, an electron-beam lithography system was employed to pattern 80-nm-wide and 980-nm-spaced multi-mesa-channel for fabricating AlGaN/GaN metal-oxide-semiconductor high electron mobility transistors (MOSHEMTs). Since the structure of multi-mesa-channel could enhance gate control capabilities and reduce the self-heating effect in the channel, the performance of the MOSHEMTs could be obviously improved. The direct current performance metrics of the multi-mesa-channel-structured MOSHEMTs, such as a saturation drain-source current of 929 mA/mm, maximum extrinsic transconductance of 223 mS/mm, and on-resistance of 2.1 Ω-mm, were much better than those of the planar-structured MOSHEMTs. Moreover, the threshold voltage of the multi-mesa-channel-structured MOSHEMTs shifted toward positive voltage from −2.6 to −0.6 V, which was attributed to the better gate control capability. Moreover, the multi-mesa-channel-structured MOSHEMTs also had superior high-frequency and low-frequency noise performance. A low Hooge's coefficient of 1.17×10^{-6} was obtained.

Keywords: electron-beam lithography system; gate control capability; metal-oxide-semiconductor high electron mobility transistors; multi-mesa-channel; photoelectrochemical etching method; self-heating effect

check for updates

Citation: Jian, J.-J.; Lee, H.-Y.; Chang, E.-Y.; Lee, C.-T. Investigation of Multi-Mesa-Channel-Structured AlGaN/GaN MOSHEMTs with SiO_2 Gate Oxide Layer. *Coatings* **2021**, *11*, 1494. https://doi.org/10.3390/coatings11121494

Academic Editor: Aomar Hadjadj

Received: 24 September 2021
Accepted: 1 December 2021
Published: 3 December 2021

1. Introduction

Recently, due to the rapid requirement of emerging applications such as electric vehicles, fifth generation (5G) wireless systems, and renewable energy systems, high-power and high-frequency devices have attracted significant attention. Although both gallium nitride (GaN)-based and silicon carbide (SiC)-based materials are used in high-power and high-frequency amplifiers [1–4], SiC is much more expensive than GaN [5]. Moreover, due to the polarization effect in the AlGaN/GaN heterostructure, a two-dimensional electron gas (2-DEG) with high sheet electron density and high electron mobility can be obtained. To improve the power-handling capabilities and enhance operation voltage by reducing gate leakage current, AlGaN/GaN metal-oxide-semiconductor high electron mobility transistors (MOSHEMTs) have been used to replace metal-semiconductor HEMTs and have become mainstream high-frequency devices and high-power devices used in various systems [6]. To fabricate AlGaN/GaN MOSHEMTs, several dielectric materials, such as SiO_2 [7–10], Si_3N_4 [11,12], Al_2O_3 [13,14], Ga_2O_3 [6,15], ZnO [16], and $LiNbO_3$ [17], have been inserted between gate metal and GaN-based semiconductors as the gate oxide layer. Of the dielectric materials, SiO_2 film is a promising gate oxide material due to its stable properties, leakage current suppression, and commonly easy deposition. By using an SiO_2 gate oxide layer, AlGaN/GaN planar-structured MOSHEMTs have been previously reported [7–10]. Despite the success of planar-structured devices, several studies have reported that gate control capability and self-heating dissipation could be improved by employing a multi-mesa-channel (MMC) structure in AlGaN/GaN MOSHEMTs [18–23]. Additionally, a gate-recessed structure has been widely employed in AlGaN/GaN MOSHEMTs to improve gate control capabilities [24]. To create gate-recessed and MMC regions, several etching techniques, such as reactive ion etching (RIE) [25,26], inductively coupled plasma RIE (ICP RIE) [2,27], neutral beam etching (NBE) [28], atomic layer etching (ALE) [1], and photoelectrochemical (PEC) etching [29,30], have been utilized and reported on previously. Compared to the aforementioned etching systems, the PEC etching system is promising due to its resulting low damage and low etching defects on etched GaN-based surfaces. To compare the performance of AlGaN/GaN planar-structured MOSHEMTs to those with SiO_2 gate oxide layers, AlGaN/GaN MMC-MOSHEMTs with SiO_2 gate oxide layers were fabricated and studied in this work. Moreover, the PEC etching method was used to create the gate-recessed and MMC structures in the fabrication of AlGaN/GaN MOSHEMTs. The related direct current (DC), high-frequency noise, and low-frequency noise properties of the AlGaN/GaN planar-structured and MMC-MOSHEMTs with SiO_2 gate oxide layers were measured and analyzed.

2. Devices Fabricated Procedure and Methods

In this study, epitaxial wafers grown on sapphire substrates by a metalorganic chemical vapor deposition (MOCVD) system were obtained from Nippon Telegraph and Telephone Advanced Technology Co. (NTT-AT), Japan. The epitaxial layers included a 20-nm-thick AlN nucleation layer, a 4-μm-thick carbon-doped GaN buffer layer, a 300-nm-thick undoped GaN (i-GaN) layer, and a 35-nm-thick AlGaN barrier layer. A 2-DEG channel with a sheet electron density of 1.1×10^{13} cm^{-2} and an electron mobility of 1700 cm^2/V-s was formed at the polarized AlGaN/GaN hetero-structured interface. Figure 1a depicts the three-dimensional schematic configuration of the AlGaN/GaN MMC-MOSHEMTs with 30-nm-thick SiO_2 gate oxide layers. Figure 1b depicts a high-resolution transmittance electron microscope (HR-TEM) image of the multi-mesa-channel. To fabricate the AlGaN/GaN MOSHEMTs, after a positive photoresist (GL-2000) was firstly spun on the samples with a spin coater, parallel nanostrip patterns with a width of 80 nm and a spacing of 980 nm were created using an electron-beam lithography system (ELS-7500). The photoelectrochemical (PEC) etching method was utilized to etch the 80-nm-wide nanostrip-patterned samples to isolate the 2-DEG channel and form a multi-mesa-channel. The PEC etching method and processes were previously discussed [29,30]. According to the HR-TEM image shown in Figure 1b, under a 50-μm-wide gate region, the total channel width of the multi-mesa-channel was approximately 3.76 μm. After an isolation mesa region (area = 310 μm × 320 μm) was patterned by a 500-nm-thick Ni metal mask, a reactive-ion etching system with a BCl_3 etchant was utilized to etch the region without Ni metal mask protection down to a depth of about 600 nm in the carbon-doped GaN buffer layer. Subsequently, an ammonium sulfide ($(NH_4)_2S_x$) chemical solution was used to treat the sample's surface at 60 °C for 30 min, which was able to completely remove the undesired native oxide residing on the surface of the AlGaN barrier layer [31].

After the surface treatment, an electron-beam evaporator was employed to sequentially deposit Ti/Al/Pt/Au (25/100/50/400 nm, respectively) laminated metals on the patterned samples as the source and drain electrodes of the MOSHEMTs. To obtain better ohmic contact performance, the samples were annealed in a nitrogen atmosphere at 850 °C for 1 min using a rapid-thermal annealing system. The separation between the source electrode and the drain electrode was 10 μm. Prior to depositing the 30-nm-thick SiO_2 gate oxide layer, a patterned gate region with a width of 50 μm and a length of 1 μm was etched about 10 nm away by PEC etching method to form the gate-recessed structure. After the surface treatment of $(NH_4)_2S_x$ chemical solution again, the 30-nm-thick SiO_2 gate oxide layer was deposited on the gate-recessed samples with a radio frequency (RF) magnetron sputtering system using an Si target (99.999%) purchased from Admat Inc., Japan. The RF power, chamber pressure, and argon/oxygen gas flow were 125 W, 10 mtorr, and 30/20 sccm, respectively. Subsequently, the gate electrode of Ni/Au (20/300 nm) metals was deposited on the SiO_2 gate oxide layer using an electron-beam evaporator. Finally, after using the lift-off technique to remove the redundant SiO_2 layer and Ni/Au metals, AlGaN/GaN MMC-MOSHEMTs with SiO_2 gate oxide layers were fabricated. The AlGaN/GaN planar-structured MOSHEMTs with a channel length of 10 µm, channel width of 50 µm, and gate length of 1 µm were also fabricated as comparison devices.

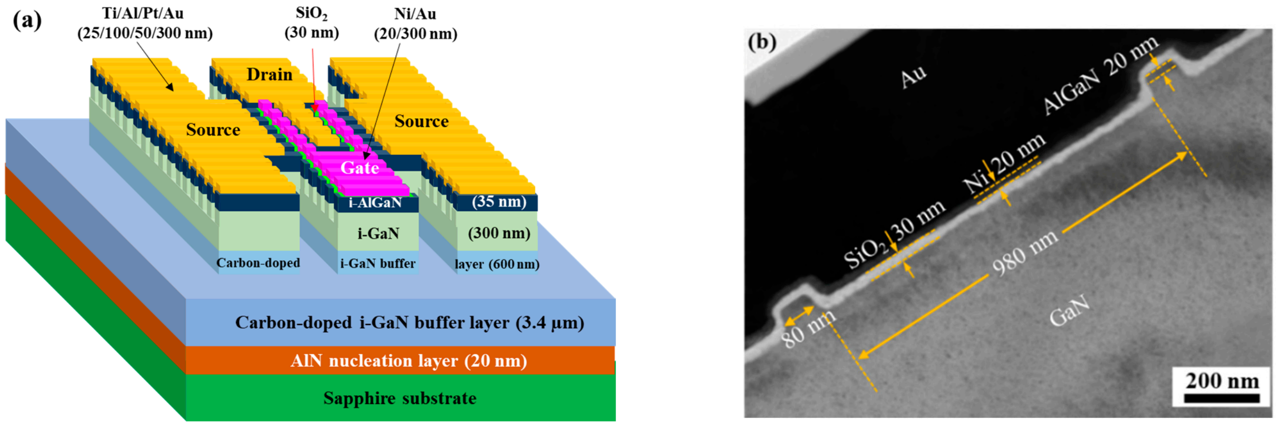

Figure 1. (**a**) Schematic configuration of AlGaN/GaN multi-mesa-channel-structured MOSHEMTs with SiO_2 gate oxide layers and (**b**) HR-TEM image of multi-mesa-channel.

3. Experimental Results and Discussion

Following the measurements of an Agilent 4156C semiconductor parameter analyzer, Figure 2a,b depicts drain-source current (I_{DS})-drain-source voltage (V_{DS}) characteristics of the AlGaN/GaN planar-structured and MMC-MOSHEMTs, respectively, operating at various gate-source voltages (V_{GS}). At the operating voltages of V_{DS} = 10 V and V_{GS} = 5 V, the saturation drain-source current (I_{DSS}) values of the planar-structured and MMC-MOSHEMTs were 475 and 929 mA/mm, respectively. Since the total real channel widths were 50 µm and 3.76 µm for the planar-structured and MMC-MOSHEMTs, respectively, the associated total real drain-source current values were 23.75 mA and 3.49 mA, respectively. After calculating the on-resistance (R_{on}) from $dV_{DS}/dI_{DS}|_{V_{DS}=0\text{ V},\ V_{GS}=5\text{ V}}$, the R_{on} values of the planar-structured and MMC-MOSHEMTs were found to be 13.9 and 2.1 Ω-mm, respectively.

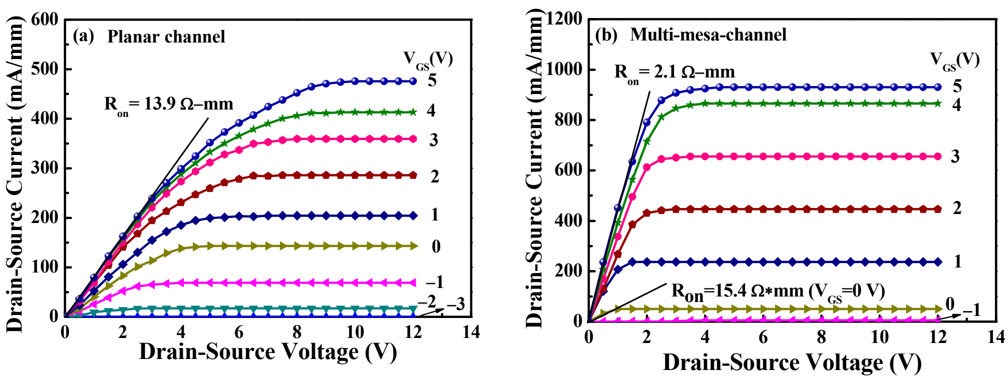

Figure 2. Drain-source current–drain-source voltage characteristics of (**a**) planar-structured MOSHEMTs and (**b**) multi-mesa-channel-structured MOSHEMTs operating at various gate-source voltages.

Figure 3a,b depicts the dependence of drain-source current and the extrinsic transconductance (g_m) on the gate-source voltage of both the MOSHEMTs operating at V_{DS} = 10 V. The maximum extrinsic transconductance (g_{mmax}) values of 79 and 223 mS/mm were obtained for the planar-structured and MMC-MOSHEMTs, respectively. Moreover, the corresponding threshold voltages (V_{TH}) were −2.6 and −0.6 V, respectively. The value of V_{TH} was defined as the V_{GS} corresponding to I_{DS} = 1 μA/mm. According to the experimental results, the direct current performance, g_{mmax}, and R_{on} of the MMC-MOSHEMTs were better than those of the planar-structured MOSHEMTs. In addition to the smaller heat-release power in the multi-mesa-channel-structured devices due to the smaller total real drain-source current, the improvement mechanisms were attributed to the fact that the lateral heat flow within the space between the multi-mesa-channel could be easily driven to achieve better heat dissipation [22,32]. Consequently, the self-heating effect could be reduced in the multi-mesa-channel structure. Moreover, compared to the planar-structured MOSHEMTs, the V_{TH} of the MMC-MOSHEMTs moved toward the positive voltage direction. This phenomenon was attributed to the better gate control capability enabled by modulation of the two additional lateral electric fields from the wall of the multi-mesa-channel, in addition to the vertical electric field modulation from the top surface [24,33]. The subthreshold swing (S.S.) values of 390.1 and 118.1 mV/dec were calculated from the slope of the logI_{DS}–V_{GS} characteristics of the devices with planar and multi-mesa-channel structures, respectively, operating at V_{DS} = 0.1 V. Due to their better gate control capability, a better S.S. was obtained for the MMC-MOSHEMTs. The gate leakage current and breakdown characteristics are shown in Figure 4. When operating at V_{GS} = −100 V, the gate leakage current values of the planar-structured and MMC-MOSHEMTs were 5.0 μA and 10.6 nA, respectively. Similar gate breakdown voltages of −490 and −498 V for the planar-structured and MMC-MOSHEMTs were obtained due to the use of the same SiO_2 gate oxide layers.

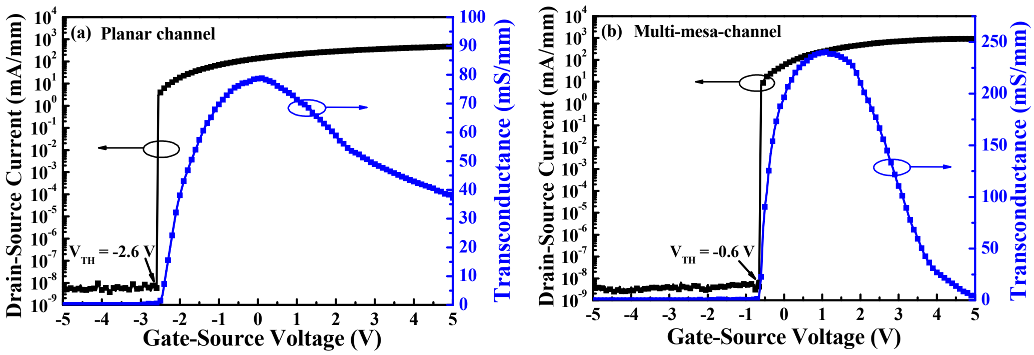

Figure 3. Drain-source current and extrinsic transconductance of (**a**) planar-structured MOSHEMTs and (**b**) multi-mesa-channel-structured MOSHEMTs.

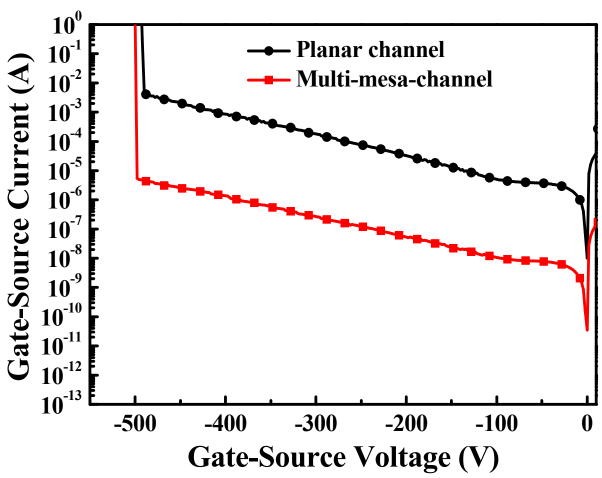

Figure 4. Gate leakage current and breakdown characteristics of planar-structured and multi-mesa-channel-structured MOSHEMTs.

To assess high-frequency performance, small-signal scattering parameters were evaluated with an Agilent 8510C network analyzer. Figure 5 presents the high-frequency performance as a function of frequency for both the MOSHEMTs operating at V_{DS} = 10 V. The unit gain cutoff frequency (f_T) and maximum frequency of oscillation (f_{max}) were, respectively, obtained from the short-circuit current gain of 0 dB and the maximum available power gain of 0 dB. For the planar-structured MOSHEMTs, the f_T and f_{max} were 4.9 and 9.4 GHz, respectively. For the MMC-MOSHEMTs, the f_T and f_{max} were 6.9 and 13.7 GHz, respectively. Compared to the high-frequency performance of the AlGaN/GaN planar-structured MOSHEMTs, the high-frequency performance was improved by using the multi-mesa-channel structure.

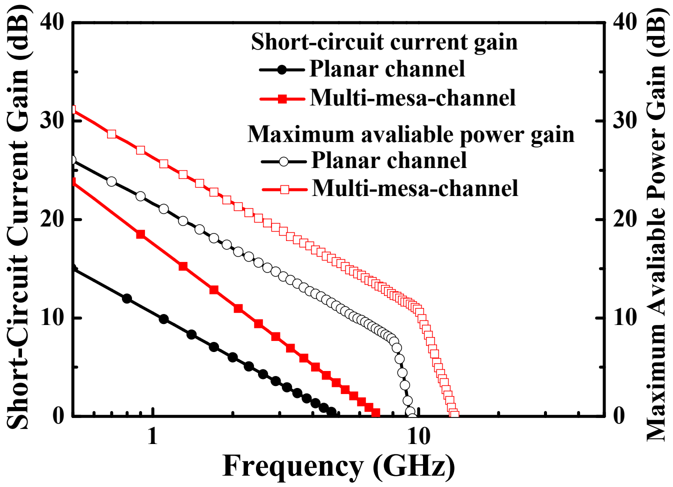

Figure 5. High-frequency performance of both MOSHEMTs as a function of frequency.

In general, the low-frequency noise performance of MOSHEMTs was significantly affected by the quality of gate oxide layer and the interface quality between gate oxide layer and semiconductor [34]. The normalized low-frequency noise power ($S_{IDS}(f)/I_{DS}^2$) spectra of both the MOSHEMTs biased at V_{DS} = 1 V and at various V_{GS} voltages were measured and are shown in Figure 6. The curves of $S_{IDS}(f)/I_{DS}^2$ for both the MOSHEMTs were well-fitted by the 1/f fitting line at the frequency range from 1 Hz to 1 kHz. Therefore, it was deduced that the dominant noise was flicker noise, which implied that low surface damage occurred on the etched gate-recessed AlGaN surface using the PEC etching method and there was good interface between the SiO_2 gate oxide layer and the gate-recessed AlGaN surface when using the $(NH_4)_2S_x$ surface treatment. The $S_{IDS}(f)/I_{DS}^2$ values of the planar-structured and MMC-MOSHEMTs biased at V_{GS} = 5 V and f = 10 Hz were 4.97×10^{-13} and 3.02×10^{-14} Hz^{-1}, respectively. Moreover, we used the mobility fluctuation model to calculate the Hooge's coefficient α, which is another important factor for appraising the low-frequency noise performance of MOSHEMTs. In general, the α value was found to be proportional to the $S_{IDS}(f)/I_{DS}^2$ and the gate width. The α values were 7.99×10^{-5} and 1.17×10^{-6} for the planar-structured and MMC-MOSHEMTs operating at V_{GS} = 5 V and f = 10 Hz, respectively. Compared to the planar structure, the MMC-MOSHEMTs had lower normalized low-frequency noise power and Hooge's coefficient values. It was indicated that better low-frequency noise performance could be achieved by using the multi-mesa-channel structure.

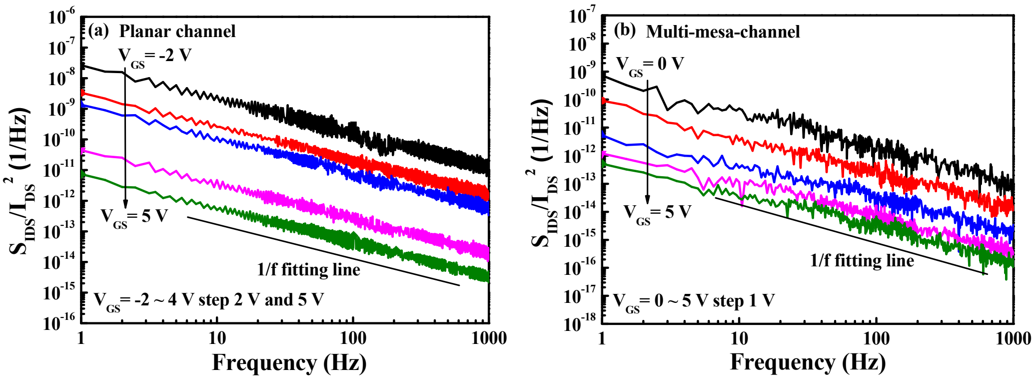

Figure 6. Normalized low-frequency noise power spectra of (**a**) planar-structured MOSHEMTs and (**b**) multi-mesa-channel-structured MOSHEMTs.

4. Conclusions

In this work, using an electron-beam lithography system and the PEC etching method, AlGaN/GaN MMC-MOSHEMTs with a gate-recessed structure and an SiO_2 gate oxide layer were manufactured. According to the improved transconductance, subthreshold swing, threshold shift, and high-frequency performance, it was deduced that the MMC-MOSHEMTs had better gate control capability and better self-heating dissipation in comparison to those of the planar-structured MOSHEMTs. Moreover, the lower normalized low-frequency noise power and Hooge's coefficient values of the MMC-MOSHEMTs confirmed that the PEC etching method and $(NH_4)_2S_x$ surface treatment could form low etching damages and defects existed on the gate-recessed AlGaN surface. Therefore, it is expected that the PEC etching method is a more suitable method and better technique for etching an AlGaN semiconductor than the reactive-ion etching system. Furthermore, according to the superior low-frequency noise performance of the planar-structured and MMC-MOSHEMTs, the SiO_2 material is a suitable gate oxide layer for fabricating AlGaN/GaN MOSHEMTs. Compared to the performance of AlGaN/GaN planar-structured and MMC-MOSHEMTs, the multi-mesa-channel is a more promising structure in various-materials-based MOS devices. However, under the same channel width, the total real drain-source current of the multi-mesa-channel-structured devices was found to be smaller than that of the planar-structured devices. Although the total real drain-source current could be enhanced by using a wider channel width, the power performance of the multi-mesa-channel-structured devices still needs work.

Author Contributions: Conceptualization, C.-T.L.; formal analysis, J.-J.J.; investigation, H.-Y.L., E.-Y.C. and C.-T.L.; data curation, J.-J.J.; writing—original draft, H.-Y.L. and C.-T.L.; writing—review and editing, H.-Y.L. and C.-T.L.; funding acquisition, C.-T.L. All authors have read and agreed to the published version of the manuscript.

Funding: This work was supported in part by the Ministry of Science and Technology of the Republic of China under Grant MOST 108-2221-E-155-029-MY3, Grant MOST 108-2221-E-006-215-MY3, and Grant MOST 109-2923-E-155-001.

Institutional Review Board Statement: Not applicable.

Informed Consent Statement: Not applicable.

Data Availability Statement: The data presented in this study are available on request from the corresponding author.

Acknowledgments: The authors appreciate the financial support from the Ministry of Science and Technology of the Republic of China.

Conflicts of Interest: The authors declare no conflict of interest.

References

1. Takakura, K.; Putcha, V.; Simoen, E.; Alian, A.R.; Peralagu, U.; Waldron, N.; Parvais, B.; Collaert, N. Low-frequency noise investigation of GaN/AlGaN metal–oxide–semiconductor high-electron-mobility field-effect transistor with different gate length and orientation. *IEEE Trans. Electron Devices* **2020**, *67*, 3062–3068. [CrossRef]
2. Huang, K.H.; Lin, Y.C.; Lee, J.H.; Hsu, C.C.; Yao, J.N.; Wu, C.Y.; Chien, C.H.; Chang, E.Y. Study of tri-gate AlGaN/GaN MOS-HEMTs for power application. *Micro. Nano. Eng.* **2020**, *9*, 100073. [CrossRef]
3. Soler, V.; Cabello, M.; Banu, V.; Jordà, X.; Montserrat, J.; Rebollo, J.; Rogina, M.R.; Mihaila, A.; Godignon, P. Reliability and robustness tests for next-generation high-voltage SiC MOSFETs. *IEEE J. Emerg. Sel. Top. Power Electron.* **2021**, *9*, 4320–4328. [CrossRef]
4. Ball, D.R.; Galloway, K.F.; Johnson, R.A.; Alles, M.L.; Sternberg, A.L.; Witulski, A.F.; Reed, R.A.; Schrimpf, R.D.; Hutson, J.M.; Lauenstein, J.M. Effects of breakdown voltage on single-event burnout tolerance of high-voltage SiC power MOSFETs. *IEEE Trans. Nucl. Sci.* **2021**, *68*, 1430–1435. [CrossRef]
5. Wang, H.Y.; Chiu, H.C.; Hsu, W.C.; Liu, C.M.; Chuang, C.Y.; Liu, J.Z.; Huang, Y.L. The impact of $Al_xGa_{1\text{-}x}N$ back barrier in AlGaN/GaN high electron mobility transistors (HEMTs) on six-inch MCZ Si substrate. *Coatings* **2020**, *10*, 570. [CrossRef]
6. Ren, F.; Hong, M.; Chu, S.N.G.; Marcus, M.A.; Schurman, M.J.; Baca, A.; Pearton, S.J.; Abernathy, C.R. Effect of temperature on $Ga_2O_3(Gd_2O_3)$/GaN metal–oxide–semiconductor field-effect transistors. *Appl. Phys. Lett.* **1998**, *73*, 3893–3895. [CrossRef]
7. Asif Khan, M.; Hu, X.; Tarakji, A.; Simin, G.; Yang, J.; Gaska, R.; Shur, M.S. AlGaN/GaN metal–oxide–semiconductor heterostructure field-effect transistors on SiC substrates. *Appl. Phys. Lett.* **2000**, *77*, 1339–1341. [CrossRef]
8. Fiorenza, P.; Greco, G.; Iucolano, F.; Patti, A.; Roccaforte, F. Channel mobility in GaN hybrid MOS-HEMT using SiO_2 as gate insulator. *IEEE Trans. Electron Devices* **2017**, *64*, 2893–2899. [CrossRef]
9. Cho, G.; Cha, H.; Kim, H. Influence of oxygen–plasma treatment on in-situ SiN/AlGaN/GaN MOSHEMT with PECVD SiO_2 gate insulator. *Materials* **2019**, *12*, 3968. [CrossRef]
10. Pang, L.; Lian, Y.; Kim, D.S.; Lee, J.H.; Kim, K. AlGaN/GaN MOSHEMT with high-quality gate–SiO_2 achieved by room-temperature radio frequency magnetron sputtering. *IEEE Trans. Electron Devices* **2012**, *59*, 2650–2655. [CrossRef]
11. Hu, X.; Koudymov, A.; Simin, G.; Yang, J.; Khan, M.A.; Tarakji, A.; Shur, M.S.; Gaska, R. Si_3N_4/AlGaN/GaN-metal-insulator-semiconductor heterostructure field-effect transistors. *Appl. Phys. Lett.* **2001**, *79*, 2832–2834. [CrossRef]
12. Chumbes, E.M.; Smart, J.A.; Prunty, T.; Shealy, J.R. Microwave performance of AlGaN/GaN metal insulator semiconductor field effect transistors on sapphire substrates. *IEEE Trans. Electron Devices* **2001**, *48*, 416–419. [CrossRef]
13. Ye, P.D.; Yang, B.; Ng, K.K.; Bude, J.; Wilk, G.D.; Halder, S.; Hwang, J.C.M. GaN metal-oxide-semiconductor high-electron-mobility-transistor with atomic layer deposited Al_2O_3 as gate dielectric. *Appl. Phys. Lett.* **2005**, *86*, 063501.
14. Liu, H.Y.; Chou, B.Y.; Hsu, W.C.; Lee, C.S.; Ho, C.S. A simple gate-dielectric fabrication process for AlGaN/GaN metal-oxide-semiconductor high-electron-mobility transistors. *IEEE Electron Device Lett.* **2012**, *33*, 997–999. [CrossRef]
15. Shih, H.Y.; Chu, F.C.; Das, A.; Lee, C.Y.; Chen, M.J.; Lin, R.M. Atomic layer deposition of gallium oxide films as gate dielectrics in AlGaN/GaN metal-oxide-semiconductor high-electron-mobility transistors. *Nanoscale Res. Lett.* **2016**, *11*, 235. [CrossRef] [PubMed]
16. Lee, C.T.; Chiou, Y.L.; Lee, C.S. AlGaN/GaN MOS-HEMTs with gate ZnO dielectric layer. *IEEE Electron Device Lett.* **2010**, *31*, 1220–1223. [CrossRef]
17. Lee, C.T.; Yang, C.L.; Tseng, C.Y.; Chang, J.H.; Horng, R.H. GaN-based enhancement-mode metal-oxide-semiconductor high-electron mobility transistors using $LiNbO_3$ ferroelectric insulator on gate-recessed structure. *IEEE Trans. Electron Devices* **2015**, *62*, 2481–2487. [CrossRef]
18. Tamura, T.; Kotani, J.; Kasai, S.; Hashizume, T. Nearly temperature-independent saturation drain current in a multi-mesa-channel AlGaN/GaN high electron mobility transistor. *Appl. Phys. Express* **2008**, *1*, 023001. [CrossRef]
19. Ohi, K.; Hashizume, T. Drain current stability and controllability of threshold voltage and subthreshold current in a multi-mesa-channel AlGaN/GaN high electron mobility transistor. *Jpn. J. Appl. Phys.* **2009**, *48*, 081002. [CrossRef]
20. Ohi, K.; Asubar, J.T.; Nishiguchi, K.; Hashizume, T. Current stability in multi-mesa-channel AlGaN/GaN HEMTs. *IEEE Trans. Electron Devices* **2013**, *60*, 2997–3004. [CrossRef]
21. Takashima, S.; Li, Z.; Chow, T.P. Sidewall dominated characteristics on fin-gate AlGaN/GaN MOS-channel-HEMTs. *IEEE Trans. Electron Devices* **2013**, *60*, 3025–3031. [CrossRef]
22. Asubar, J.T.; Yatabe, Z.; Hashizume, T. Reduced thermal resistance in AlGaN/GaN multi-mesa-channel high electron mobility transistors. *Appl. Phys. Lett.* **2014**, *105*, 053510. [CrossRef]
23. Jia, J.J.; Lin, C.C.; Lee, C.T. Scaling effect in gate-recessed AlGaN/GaN fin-nanochannel array MOSHEMTs. *IEEE Access* **2020**, *8*, 158941–158946. [CrossRef]
24. Lee, C.T.; Juo, H.Y. Multiple-submicron channel array gate-recessed AlGaN/GaN fin-MOSHEMTs. *IEEE J. Electron. Devices Soc.* **2018**, *6*, 183–188. [CrossRef]
25. Chen, C.H.; Keller, S.; Haberer, E.D.; Zhang, L.; DenBaars, S.P.; Hu, E.L.; Mishra, U.K.; Wu, Y. Cl_2 reactive ion etching for gate recessing of AlGaN/GaN field-effect transistors. *J. Vac. Sci. Technol. B* **1999**, *17*, 2755–2758. [CrossRef]
26. Qhalid Fareed, R.S.; Hu, X.; Tarakji, A.; Deng, J.; Gaska, R.; Shur, M.; Khan, M.A. High-power AlGaN/InGaN/AlGaN/GaN recessed gate heterostructure field-effect transistors. *Appl. Phys. Lett.* **2005**, *86*, 143512. [CrossRef]

27. Liu, H.Y.; Lin, C.W.; Hsu, W.C.; Lee, C.S.; Chiang, M.H.; Sun, W.C.; Wei, S.Y.; Yu, S.M. Integration of gate recessing and in situ Cl^{-} doped Al_2O_3 for enhancement-mode AlGaN/GaN MOSHEMTs fabrication. *IEEE Electron Device Lett.* **2017**, *38*, 91–94. [CrossRef]
28. Lin, Y.K.; Noda, S.; Huang, C.C.; Lo, H.C.; Wu, C.H.; Luc, Q.H.; Chang, P.C.; Hsu, H.T.; Samukawa, S.; Chang, E.Y. High-performance GaN MOSHEMTs fabricated with ALD Al_2O_3 dielectric and NBE gate recess technology for high frequency power applications. *IEEE Electron Device Lett.* **2017**, *38*, 771–774. [CrossRef]
29. Lee, H.Y.; Lin, C.H.; Wei, C.C.; Yang, J.C.; Chang, E.Y.; Lee, C.T. AlGaN/GaN enhancement-mode MOSHEMTs utilizing hybrid gate-recessed structure and ferroelectric charge trapping/storage stacked $LiNbO_3$/HfO_2/Al_2O_3 structure. *IEEE Trans. Electron Devices* **2021**, *68*, 3768–3774. [CrossRef]
30. Lee, C.T.; Lee, H.Y.; Chang, J.H. Integrated monolithic inverter using gate-recessed GaN-based enhancement-mode and depletion-mode metal-oxide-semiconductor high-electron mobility transistors. *ECS J. Solid State Sci. Technol.* **2017**, *6*, Q123–Q126. [CrossRef]
31. Chiou, Y.L.; Lee, C.S.; Lee, C.T. AlGaN/GaN metal-oxide-semiconductor high-electron mobility transistors with ZnO gate layer and $(NH4)_2S_x$ surface treatment. *Appl. Phys. Lett.* **2010**, *97*, 032107. [CrossRef]
32. Mikulics, M.; Kordo, P.; Fox, A.; Koäan, M.; Láth, H.; Sofer, Z.; Hardtdegen, H. Efficient heat dissipation in AlGaN/GaN heterostructure grown on silver substrate. *Appl. Mater. Today* **2017**, *7*, 134–137. [CrossRef]
33. Lu, B.; Matioli, E.; Palacios, T. Tri-gate normally-off GaN power MISFET. *IEEE Electron Device Lett.* **2012**, *33*, 360–362. [CrossRef]
34. Vertiatchikh, A.V.; Eastman, L.F. Effect of the surface and barrier defects on the AlGaN/GaN HEMT low-frequency noise performance. *IEEE Electron Device Lett.* **2003**, *24*, 535–537. [CrossRef]